Phys. Status Solidi B **246**, No. 2, 289–292 (2009) / **DOI** 10.1002/pssb.200880304

physica status solidi b
www.pss-b.com
basic solid state physics

Entangled photons from quantum dot devices: efficiency of post-selection

Marek Seliger[*, 1], **Ulrich Hohenester**[1], **and Gernot Pfanner**[2]

[1] Institut für Physik, Karl-Franzens-Universität Graz, Universitätsplatz 5, 8010 Graz, Austria
[2] Max-Planck-Institut für Eisenforschung, Max-Planck-Straße 1, 40237 Düsseldorf, Germany

Received 21 May 2008, revised 24 June 2008, accepted 27 October 2008
Published online 2 December 2008

PACS 42.50.Dv, 63.22.–m, 71.35.–y, 78.67.Hc

[*] Corresponding author: e-mail marek.seliger@uni-graz.at, Phone: +43-316-3805230, Fax: +43-316-3809820

We theoretically investigate the production of polarization-entangled photons through the biexciton cascade decay in a single semiconductor quantum dot. A biexciton radiatively decays through two intermediate exciton states, where polarization-entangled photons are emitted if the two decay paths differ in polarization but are indistinguishable otherwise. This ideal performance is usually spoiled by the electron–hole exchange interaction splitting the intermediate exciton states by a small amount and consequently attaching a which-path information to the photon frequencies. We discuss post-selection schemes to mask this which-path information to an outside observer. We show how spectral filtering and time shifts at a single photon level affect the photon state. Here the solid state environment plays a crucial role in the effective measurement of intermediate exciton states. Evaluating our analytical results with realistic quantum dot parameters we quantify the applicability of suggested protocols for solid-state based quantum cryptography. Our results indicate, that a high degree of entanglement is only reached by spectral alignment of the exciton states.

1 Introduction Photons emitted from single semiconductor quantum dots show interesting quantum properties. Recombination of a single exciton (an electron–hole pair) emits a single photon. A well controlled excitation process emits single photons on demand. This allows to realize a completely new type of experiments, as for example single-photon interferometer measurements [1, 2]. Alternatively, two photons emitted successively can be made indistinguishable and thus time-bin entangled [3]. The interesting quantum property of two photons emitted in the recombination of a biexciton (two excitons) is entanglement [4], the major building block for quantum communication and quantum computing [5, 6].

By optical pumping [7–9] or electrical injection of carriers [4, 10] the system is initially prepared in the biexciton state. A biexciton, consisting of two electron–hole pairs with opposite spin orientations, decays radiatively through two intermediate exciton states (see Fig. 1 for a schematic picture). If these are degenerate, the two decay paths differ in polarization but are indistinguishable otherwise leading to polarization-entangled photons. However, the electron–hole exchange interaction splits the intermediate exciton states by a small amount and encodes a which-path information to the photon frequencies, which consecutively reduces the entanglement.

In this paper we investigate strategies brought up in the literature to recover entanglement despite the exciton fine-structure splitting. First, the states can be brought back to degeneracy by means of external magnetic [8, 11, 12] or electric fields [13]. Alternatively, post-selection can be used to select only those photons whose energy contains no which-path information [9] or entangle photons produced in different generations of the decay process [14, 15].

As we will show, only the first protocol provides a viable means for reaching a high degree of entanglement. The other two inherently suffer from dephasing processes in the solid, which are always significant, and the degree of entanglement will consequently remain rather low. This paper is organized as follows. We first describe the theoretical model in Section 2, and then evaluate analytical results for two post-selection schemes with realistic quantum dot parameters in Section 3. Section 4 discusses the applicability of different post-selection strategies to accomplish a high degree of entanglement.

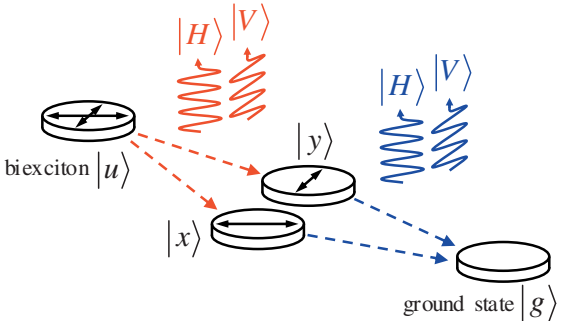

Figure 1 (online colour at: www.pss-b.com) Schematic of emission of polarization-entangled photons in biexciton cascade decay. The biexciton, consisting of two excitons with different dipole moments (indicated as arrows), decays via two paths. Depending on the path, the emitted photons have different polarization, horizontal (H) or vertical (V).

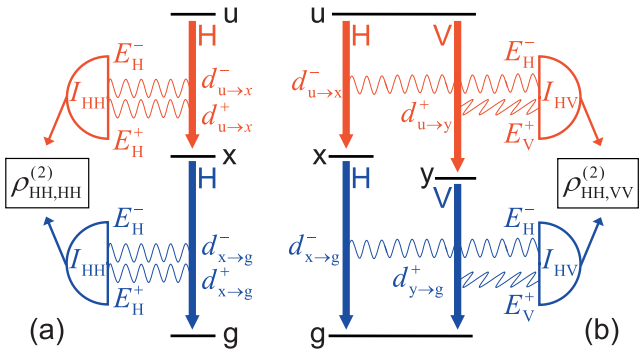

Figure 2 (online colour at: www.pss-b.com) From quantum dot dynamics to photon quantum properties: (a) Photon counting: $\rho^{(2)}_{HH,HH}$. The biexciton u decays radiatively into the x-polarized exciton (red) and successively into the ground state g (blue). The dipole operators associated with these transitions, $d^{\pm}_{u\to x}$ and $d^{\pm}_{x\to g}$, create the electric field amplitudes $E^{\pm}_H$. Photo detectors (indicated by half circles) measure the intensity I_{HH} of constructive interference of the two electric field amplitudes. $\rho^{(2)}_{HH,HH}$ is the correlation between the two measurements averaged over the photon detection times. (b) From coherent quantum dot dynamics to photon entanglement: $\rho^{(2)}_{HH,VV}$. The biexciton decays into a coherent superposition of the x- and y-polarized excitons. The two dipole operators $d^-_{u\to x}$ and $d^+_{u\to y}$ create electric field amplitudes, E^-_H and E^+_V, with different polarization (indicated by different orientation of wiggles). Due to the constant time delay between emission and detection, the two dipole operators related to an intensity I_{HV} act at the same time.

2 Theoretical model: from quantum dot dynamics to photon properties We consider the quantum dot level scheme as shown in Fig. 1 with the biexciton u, the two differently polarized excitons x and y and the ground state g. Emitted photons are polarized horizontally (H) or vertically (V). The energy of the biexciton is lowered by typically a few meV by the biexciton binding energy Δ. Therefore the first photon is red shifted allowing for a spectral discrimination. The excitons are split in energy by the fine-structure splitting δ of typically few tens of μeV.

The quantum properties of emitted photons are quantified by the two-photon density matrix $\rho^{(2)}$ in the basis of polarization, H and V, which is obtained in experiments by quantum state tomography. We assume that the quantum dot is placed into a weakly coupling cavity, allowing for emission into well defined polarization states. $\rho^{(2)}$ is the average over the detection time of the photon intensities at the two detectors

$$\rho^{(2)} = \mathrm{avg}\left[\left\langle :\hat{I}(t_r)\,\hat{I}(t_b):\right\rangle\right], \tag{1}$$

of the first red photon at time t_r and the second blue photon at time t_b. The intensity operator is the interference of two electric field amplitude operators $\hat{I}(t) = \hat{E}^-(t)\,\hat{E}^+(t)$ at the photon detector. Plus or minus denote the positive or negative frequency component. Each electric field amplitude operator is created by a dipole operator of an excitonic transition. For example, $\hat{E}^-_H(t_r)$ is created by the dipole $\hat{d}^-_{u\to x}(t_r)$ describing the biexciton decay into x. The propagation of the photon from emission to the detector introduces only a constant time delay, which is equal for all photons and omitted in the following.

Figure 2 illustrates the construction of $\rho^{(2)}$. Since spin flips ($x \to y$) are negligible, only 4 elements of $\rho^{(2)}$ are nonzero. We find $\rho^{(2)}_{HH,HH} = \rho^{(2)}_{VV,VV} = 1/2$ which are the overall probabilities for one of the biexciton decay paths and $\rho^{(2)}_{HH,VV} = (\rho^{(2)}_{VV,HH})^*$. The degree of entanglement is then conveniently expressed by the concurrence [16] which in this case is $C = |\rho^{(2)}_{HH,VV}|/\rho^{(2)}_{HH,HH}$. We find complete entanglement for $C = 1$ and no entanglement for $C = 0$.

To describe the average in (1) we apply the quantum regression theorem [17–19] which allows to calculate time averages by unraveling the dynamics of the exciton density matrix ρ into two parts: (i) discontinuous quantum jumps mediated by the radiative decay as described by the dipole operators and (ii) a continuous time evolution in between. The relative phase between the dipole operators depends on the phases acquired during the continuous time evolution. These phases are transferred to the electric field amplitudes which determine the interference signal at the detector.

We find that the phases φ that ρ_{ij} acquires (see Fig. 3) are given by three components: (i) the energy difference between the two states i and j, (ii) the radiative relaxation rate γ_R of typically 1.6 μeV and (iii) dephasing γ_D due to coupling to the solid state environment for i and j with different exciton numbers. Cross dephasing [20, 12] which is not considered here, would also affect states with equal exciton numbers. In the rotating frame picture φ_{ij} for $i = j$ depends only on γ_R.

The relative phase acquired by the left decay path (i.e. $\rho_{uu} \to \rho_{xx} \to \rho_{gg}$) is then $\varphi = -2\gamma_R t_r - \gamma_R(t_b - t_r)$ where $t_b - t_r$ is the time spent in the intermediate state. The decay via two paths, $\rho_{uu} \to \rho_{xy} \to \rho_{gg}$, gives $\varphi = -2\gamma_R t_r + (-i\delta - \gamma_R)(t_b - t_r)$. Averaging over the detec-

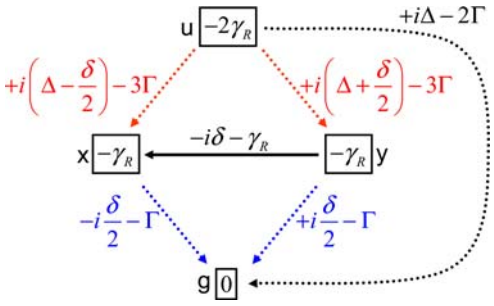

Figure 3 (online colour at: www.pss-b.com) Phase acquired within the quantum regression theorem. Density matrix elements acquire a phase $\exp(i\varphi\tau)$ between discrete jumps where τ denotes the time interval spent in this state. φ itself is per unit time and we use $\Gamma=(\gamma_R+\gamma_D)/2$. Phases in boxes are acquired for diagonal elements (i.e. $\varphi=-2\gamma_R$ for ρ_{uu}) while phases along arrows are acquired for off-diagonal elements of ρ (i.e. $\varphi=-i\delta-\gamma_R$ for ρ_{xy}) where index order is indicated by arrow direction. Solid line: phase of superposition of states with equal exciton number as relevant for the unfiltered emission. Dotted lines: phase for unequal exciton numbers.

tion times t_r and t_b we obtain the degree of entanglement

$$C=|(1+i\delta/\gamma_R)^{-1}|. \tag{2}$$

For typical fine-structure splitting of few tens of μeV the concurrence is considerably reduced as indicated by solid line in Fig. 5(a). Here a which-path information is encoded in the photon spectrum, such that an outside observer could obtain the path information by a frequency measurement.

3 Post-selection: filter and time reordering The degree of entanglement can be increased by selecting only photons with no spectral information. However, perfect entanglement can be only achieved by a filter with a width $\delta\omega\to 0$. To quantify the degree of entanglement for filters with a finite width, we reconsider the action of a filter on $\rho^{(2)}$. The photon intensity is obtained from

$$\hat{I}_{\mathrm{HV}}(t)=\hat{E}^-_{\mathrm{H}}(t)\,\hat{E}^+_{\mathrm{V}}(t)\propto\int_0^t \mathrm{d}t_1 h(t-t_1)\int_0^t \mathrm{d}t_2\; h(t-t_2)$$
$$\times\,\hat{d}^-_{u\to x}(t_1)\,\hat{d}^+_{u\to y}(t_2), \tag{3}$$

with h being the filter function of Lorentzian shape in energy domain. Equation (3) describes how the photon wave packet propagates away from the dot and becomes modulated by the filter (see Fig. 4). Due to the extraction of frequency information from the temporal field evolution, the intensity $\hat{I}_{\mathrm{HV}}(t)$ is determined by interference of dipoles emitting at different times. For a spectral width large in comparison to the excitonic linewidth (Fig. 4(b)), the filter function becomes delta-like in time, and one recovers the unfiltered case. Contrary, for a narrowband filter (Fig. 4(c)) the integrals extend over a considerable time interval of the emission process.

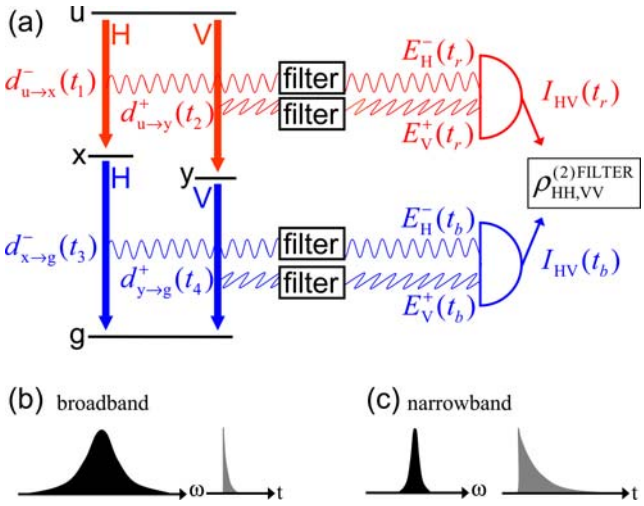

Figure 4 (online colour at: www.pss-b.com) (a) Calculation of the two-photon density matrix with a spectral filter. The action of the filter for each amplitude is the convolution with the filter function over a time interval. The emitting dipole operators can act at different times, $d^-_{u\to x}(t_1)$ and $d^+_{u\to y}(t_2)$ and analogous for the second photon. (b) Spectral width of a broadband filter with the corresponding narrow time distribution. This filter allows only for contribution to $I_{\mathrm{HV}}(t_r)$ with $t_1\approx t_2$. (c) Narrowband filter with a wide time distribution. Here also dipoles where $t_1\neq t_2$ contribute to $I_{\mathrm{HV}}(t_r)$.

Cascades contributing to $\rho^{(2)}$ evolve like (see Fig. 4) $\rho_{uu}\to\rho_{xu}\to\rho_{xy}\to\rho_{gy}\to\rho_{gg}$ which involves also superpositions of states with unequal exciton numbers. Then phases contributing to $\rho^{(2)}$ contain also terms depicted by dotted lines in Fig. 3. Here the dephasing by the solid state environment enters through γ_D. In Fig. 5(a) we present numerical results for typical quantum dot parameters. We observe two trends: the filter increases the degree of entanglement especially for $\delta\omega\ll\delta$. However, solid state dephasing considerably reduces the concurrence for realistic phonon dephasing rates of 2–5 μeV.

A recent proposal [14, 15] for post-selecting entangled photons is based on the fact that in quantum dots with zero biexciton binding energy the photons from $u\to x$ and $y\to g$ are emitted at equal energy. The idea is to entangle the $u\to x/y\to g$ photon with the $u\to y/x\to g$ photon, and to create an anticorrelated $|\mathrm{HV}\rangle+|\mathrm{VH}\rangle$ Bell state. This entanglement over generations of photons requires a time delay (t_0) of the first photon in order to increase the overlap with the second generation photon.

The intensity of the red photon is then determined by $\hat{I}_{\mathrm{HV}}(t_r)\propto\hat{d}^-_{u\to x}(t_1-t_0)\,\hat{d}^+_{y\to g}(t_2)$ and of the blue photon by $\hat{I}_{\mathrm{HV}}(t_b)\propto\hat{d}^-_{u\to y}(t_3-t_0)\,\hat{d}^+_{x\to g}(t_4)$. The crucial point here is, that the phase relation between the two dipoles building up the interference intensity is determined by the time difference at the creation time of the field amplitude, i.e. t_2-t_1. This can be much larger than the average arrival time at the detector, $t_2-t_0-t_1$, that can be tuned to zero. In the long time interval t_2-t_1, dephasing can be very effective. Evaluating this scheme within the above described model

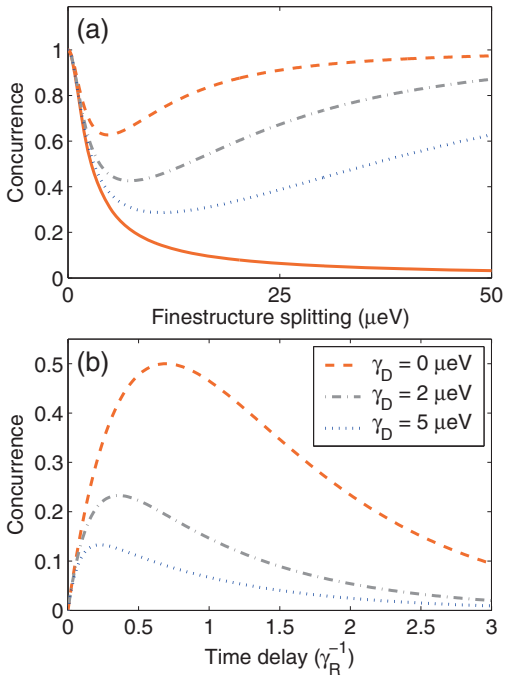

Figure 5 (online colour at: www.pss-b.com) (a) Concurrence with a spectral filter ($\delta\omega = 1\,\mu$eV) as a function of fine-structure splitting δ and parametrized for different dephasing rates γ_D. Solid line: data calculated without a filter. (b) Concurrence with time reordering of generations as a function of time delay t_0 for different dephasing rates.

we obtain for the degree of entanglement

$$C = \frac{e^{-\gamma_R t_0} - e^{-2(\gamma_R+\gamma_D)t_0}}{1/2 + \gamma_D/\gamma_R}, \qquad (4)$$

which is also numerically evaluated in Fig. 5(b). Ignoring solid state effects ($\gamma_D = 0$), we obtain a maximal concurrence of 1/2. Additionally, the solid state environment is effective for dephasing already for γ_D of 2–5 μeV.

4 Conclusions We have presented a quantitative description of photon entanglement generation in a biexciton cascade decay. We used these results to evaluate recent schemes for post-selection of entangled photons. Spectral filtering on the one hand masks the which-path information to an outside observer, but on the other hand introduces a strong sensitivity to solid state induced dephasing. An alternative approach of entangling photons from different generations does not only suffer in the same way from solid state dephasing, but also from dephasing due to a large time difference between the creation of interfering field amplitudes.

In general, we have demonstrated that a spectral filter and time reordering significantly modify the quantum information encoded in the two-photon wave packet. These results suggest, that the considered post-selection schemes do not seem promising to reach a high degree of entanglement in practice. The crucial aspect in constructing a post-selection scheme is the relative phase of the dipoles creating the field amplitudes that interfere at the photo detector. Long time intervals between emission clearly increase fluctuations of this phase and consequently the sensitivity to dephasing. We conclude that the most promising strategy is to energetically align the two exciton levels and thus avoid time jitter of photon amplitude emission.

References

[1] C. Santori, D. Fattal, J. Vuckovic, G. S. Solomon, and Y. Yamamoto, Nature (London) **419**, 594 (2002).
[2] C. Santori, D. Fattal, J. Vuckovic, G. S. Solomon, and Y. Yamamoto, Fortschr. Phys. **52**, 1180 (2004).
[3] M. Largu, A. Beveratos, and I. Robert-Philip, Eur. Phys. J. D **47**, 119 (2008).
[4] O. Benson, C. Santori, M. Pelton, and Y. Yamamoto, Phys. Rev. Lett. **84**, 2513 (2000).
[5] E. Knill, R. Laamme, and G. J. Milburn, Nature **409**, 46 (2001).
[6] N. Gisin, G. Ribordy, W. Tittel, and H. Zbinden, Rev. Mod. Phys. **74**, 145 (2002).
[7] P. Michler, A. Kiraz, C. Becher, W. V. Schoenfeld, P. M. Petroff, L. Zhang, E. Hu, and A. Imamoglu, Science **290**, 2282 (2000).
[8] R. M. Stevenson, R. J. Young, P. Atkinson, K. Cooper, D. A. Ritchie, and A. J. Shields, Nature (London) **439**, 179 (2006).
[9] N. Akopian, N. H. Lindner, E. Poem, Y. Berlatzky, J. Avron, D. Gershoni, B. D. Gerardot, and P. M. Petroff, Phys. Rev. Lett. **96**, 130501 (2006).
[10] Z. Yuan, B. E. Kardynal, R. M. Stevenson, A. J. Shields, C. J. Lobo, K. Cooper, N. S. Beattie, D. A. Ritchie, and M. Pepper, Science **295**, 102 (2002).
[11] R. J. Young, R. M. Stevenson, P. Atkinson, K. Cooper, D. A. Ritchie, and A. J. Shields, New J. Phys. **8**, 29 (2006).
[12] A. J. Hudson, R. M. Stevenson, A. J. Bennett, R. J. Young, C. A. Nicoll, P. Atkinson, K. Cooper, D. A. Ritchie, and A. J. Shields, Phys. Rev. Lett. **99**, 266802 (2007).
[13] B. D. Gerardot, S. Seidl, P. A. Dalgarno, R. J. Warburton, D. Granados, J. M. Garcia, K. Karrai, A. Badolato, and P. M. Petroff, Appl. Phys. Lett. **90**, 041101 (2007).
[14] M. E. Reimer et al., Voltage induced hidden symmetry and photon entanglement generation in a single site-selected quantum dot, arXiv:0706.1075 (2007).
[15] J. E. Avron, G. Bisker, D. Gershoni, N. H. Lindner, E. A. Meirom, and R. J. Warburton, Phys. Rev. Lett. **100**, 120501 (2008).
[16] W. K. Wooters, Phys. Rev. Lett. **80**, 2245 (1998).
[17] L. Mandel and E. Wolf, Optical Coherence and Quantum Optics (Cambridge University Press, Cambridge, 1995).
[18] C. W. Gardiner and P. Zoller, Quantum Noise (Springer, Berlin, 2004).
[19] G. Pfanner, M. Seliger, and U. Hohenester, Phys. Rev. B **78**, 195410 (2008).
[20] U. Hohenester, G. Pfanner, and M. Seliger, Phys. Rev. Lett. **99**, 047402 (2007).

